Hepatocyte-Specific IKKβ Expression Aggravates Atherosclerosis Development in *APOE*3-Leiden* Mice

Man C. Wong[1,2], Janna A. van Diepen[1], Lihui Hu[1], Bruno Guigas[3], Hetty C. de Boer[4,5], Gijs H. van Puijvelde[7], Johan Kuiper[7], Anton J. van Zonneveld[4,5], Steven E. Shoelson[8], Peter J. Voshol[1,a], Johannes A. Romijn[1,b], Louis M. Havekes[1,6,9], Jouke T. Tamsma[1], Patrick C.N. Rensen[1], Pieter S. Hiemstra[2], Jimmy F.P. Berbée[1,10]

Depts. of [1]Endocrinology and Metabolic Diseases, [2]Pulmonology, [3]Molecular Cell Biology, [4]Nephrology, [5]Einthoven Laboratory for Experimental Vascular Medicine, [6]Dept. of Cardiology Leiden University Medical Center, Leiden, The Netherlands; [7]Division of Biopharmaceutics, Leiden/Amsterdam Center for Drug Research, Gorlaeus Laboratories, Leiden, The Netherlands; [8]Joslin Diabetes Center and the Dept. of Medicine, Boston, USA; [9]Netherlands Organization for Applied Scientific Research – Biosciences, Gaubius Laboratory, Leiden, The Netherlands; [10]Dept. of Experimental Immunohematology, Sanquin Research Amsterdam, Amsterdam, The Netherlands; [a]Present address: Metabolic Research Laboratories, Institute of Metabolic Science, Addenbrooke's Hospital Cambridge, United Kingdom; [b]Present address: Dept. of Internal Medicine, University of Amsterdam, Amsterdam, The Netherlands

Atherosclerosis 2012;220(2):362-368

Abstract

The liver is the key organ involved in systemic inflammation, but the relation between hepatic inflammation and atherogenesis is poorly understood. Since nuclear factor-κB (NF-κB) is a central regulator of inflammatory processes, we hypothesized that chronically enhanced hepatic NF-κB activation, through hepatocyte-specific expression of IκB kinase-β (IKKβ) (*LIKK*), will aggravate atherosclerosis development in *APOE*3-Leiden (E3L*) mice. *E3L.LIKK* and *E3L* control littermates were fed a Western-type diet for 24 weeks. *E3L.LIKK* mice showed a 2.3-fold increased atherosclerotic lesion area and more advanced atherosclerosis in the aortic root with less segments without atherosclerotic lesions (11 *vs*. 42%), and more segments with mild (63% *vs*. 44%) and severe (26% *vs*. 14%) lesions. Expression of *LIKK* did not affect basal levels of inflammatory parameters, but plasma cytokine levels tended to be higher in *E3L.LIKK* mice after lipopolysaccharide (LPS) administration. *E3L.LIKK* mice showed transiently increased plasma cholesterol levels, confined to (V)LDL. This transient character resulted in a mild (+17%) increased cumulative plasma cholesterol exposure. We conclude that selective activation of NF-κB in hepatocytes considerably promotes atherosclerosis development which is (at least partly) explained by an increased sensitivity to pro-inflammatory triggers and transiently increased plasma cholesterol levels.

Introduction

Increased inflammation, in addition to disturbances in lipid metabolism, is the other main contributor to the development of atherosclerosis.[1] Nuclear factor-κB (NF-κB) has been identified as the most important transcription factor in the regulation of inflammatory processes during atherosclerosis development.[2] In unstimulated cells, NF-κB p65/p50 dimer is kept inactive by its inhibitory protein: inhibitor of κB (IκB). A wide range of extracellular stimuli, including cytokines, microbial components, and also free fatty acids, induce activation of the IκB kinase complex, which consists of two kinases (IKKα and -β) and a regulatory subunit, NEMO/IKKγ. This complex mediates the phosphorylation of IκB, resulting in its ubiquitination and degradation, leaving the NF-κB dimer free to translocate to the nucleus and activate its target genes.[2]

While general inhibition of the NF-κB pathway by pharmacological agents reduces atherosclerosis development in mice,[3, 4] the relative contribution of NF-κB may differ at cellular- or tissue-specific level. Suppression of the NF-κB pathway in endothelial cells by ablation of NEMO/IKKγ has been shown to decrease atherosclerosis development.[5] In murine bone marrow transplantation models, inhibition of the NF-κB pathway at distinct levels in hematopoietic cells can have different outcomes, *i.e.* deficiency of the NF-κB p50 subunit resulted in smaller atherosclerotic lesions,[6] whereas deletion of IKKβ increased atherosclerosis development.[7] Surprisingly, the role of the NF-κB pathway in hepatocytes on atherosclerosis development has not been investigated thus far.

The liver plays a central role in both lipid metabolism[8] and inflammation.[9] Disturbances in lipid metabolism and increased inflammation are the two main risk factors for atherogenesis.[1] Hepatocytes form the largest population of cells in the liver and execute most of its important functions. During inflammation, acute phase proteins are mainly synthesized by the hepatocytes.[10] Interestingly, hepatocyte-specific deficiency of gp130, a receptor component of IL-6 signaling which signals independent of the NF-κB pathway, decreases atherosclerosis in *apoe*$^{-/-}$ mice,[11] suggesting that reduced hepatic inflammation is associated with less atherosclerosis development.

Despite ample evidence implicating the involvement of NF-κB in atherogenesis, the hepatocyte-specific role of NF-κB in atherosclerosis has not been investigated directly. Therefore, in this study we aimed to investigate whether chronic activation of hepatocyte-specific NF-κB aggravates atherosclerosis development. We used transgenic mice with hepatocyte-specific expression of human IKKβ (Liver-specific IKKβ or *LIKK* mice), resulting in an increase of active NF-κB,[12] crossbred with atherosclerosis-prone *APOE*3-Leiden* (*E3L*) mice. *E3L* mice exhibit a human-like lipoprotein distribution on a cholesterol-rich diet due to transgenic expression of a human mutant of the *APOE3* gene, and are therefore susceptible to atherosclerosis development.[13] Collectively, our results show that hepatocyte-specific NF-κB activation markedly aggravates atherosclerosis development in *E3L* mice.

Methods

Animals and study design

Transgenic *LIKK* mice expressing constitutively active human IKKβ in the hepatocytes by an albumin promoter[12] were crossbred with *E3L* mice[14] to generate heterozygous *E3L.LIKK* and control *E3L* littermates, as described before.[15] Mice were housed under standard conditions with a 12-hour light/dark cycle and had free access to food and water. Female mice of 10-12 weeks of age were fed a Western-type diet containing 15% (w/w) cacao butter supplemented with 0.25% (w/w) cholesterol (Hope Farms, Woerden, The Netherlands). Food intake and body weight were measured weekly. Unless indicated otherwise, blood was drawn every 4 weeks after 4 hours of fasting in EDTA-containing tubes by tail bleeding, and plasma was isolated by centrifugation. All animal experiments were approved by the Institutional Ethical Committee on Animal Care and Experimentation of the Leiden University Medical Center (Leiden, The Netherlands).

mRNA expression analysis

Total RNA from livers of *E3L* and *E3L.LIKK* mice was isolated using an RNA isolation kit according to manufacturer's specifications, including a 15 min. DNAse I treatment (Macherey-Nagel, Düren, Germany). Quality control of the isolated RNA was checked with the lab-on-a-chip technology using Experion Stdsens analysis kit (Bio-Rad, Hercules, CA). One µg of total RNA was converted to cDNA with iScript cDNA Synthesis kit (Bio-Rad) and purified with Nucleospin Extract II kit (Macherey-Nagel, Düren, Germany). Real time PCR (RT-PCR) was carried out on an iQ5 Single-Color real-time PCR detection system (Bio-Rad) using the Sensimix SYBR Green RT-PCR mix (Quantace, London, UK). Expression levels were normalized using hypoxanthine-guanine phosphoribosyl transferase (*Hprt*), cyclophilin (*Cyclo*) and glyceraldehyde 3-phosphate dehydrogenase (*Gapdh*). Primer sequences are listed in Supplemental Table 1.

Western blot analysis

Liver tissue was homogenized by Ultraturrax (22,000 rpm; 2x5 sec) in an ice-cold buffer (pH 7.4) containing 30 mM Tris.HCl, 150 mM NaCl, 10 mM NaF, 1 mM EDTA, 1 mM Na_3VO_4, 0.5% (v/v) Triton X-100, 1% (v/v) SDS and protease inhibitors (Complete, Roche, Mijdrecht, The Netherlands) at a 1:6 (w/v) ratio. Homogenates were centrifuged (16,000 rpm; 15 min., 4°C) and the protein content of the supernatant was determined using the BCA protein assay kit (Pierce, Rockford, IL). Proteins (20-50 µg) were separated by 7-10% SDS-PAGE followed by transfer to a polyvinylidene fluoride membrane. Membranes were blocked for 1 hour at room temperature in Tris-buffered saline with Tween-20 with 5% non-fat dry milk followed by an overnight incubation with either IKKβ (ab32135, Abcam, Cambridge, UK), tubulin, pSer536 NF-κB p65 or NF-κB p65 antibodies (#2148, #3031, #3034, resp., Cell Signaling, Danvers, MA). Blots were then incubated with horseradish peroxidase-conjugated secondary antibodies for 1 hour at room temperature. Bands were visualized by enhanced chemiluminescence and quantified using Image J software (NIH, USA).

Plasma inflammatory markers

Plasma levels of serum amyloid A (SAA) were determined using the murine Phase Serum Amyloid A Assay kit (Tridelta, County Kildare, Ireland) according to manufacturer's instructions. Plasma levels of inflammatory cytokines and chemokines (IFNγ, IL-12 p70, IL-1β, IL-6, TNFα and IL-10) were measured using a multiplex murine inflammatory cytokine profile immunoassay from Meso Scale Discovery (MSD) on a MSD 2400 plate reader according to the manufacturer's protocol (MSD, Gaithersburg, MD).

Lipopolysaccharide stimulation

Mice were injected i.v. with *Salmonella minnesota* Re595 lipopolysaccharide (LPS) (Sigma-Aldrich, St. Louis, MO) (50 mg/kg body weight). Blood was collected 90 min. after injection in heparin-coated capillaries. Plasma was assayed for cytokines as described above.

FACS staining of leukocyte subpopulations in peripheral blood

Nonfasted, whole blood was drawn in EDTA-containing tubes by tail bleeding and incubated with antibodies against Ly6C-FITC (kindly provided by dr P.J. Leenen, Erasmus University, Rotterdam, The Netherlands), Ly6G-PE, CD115-biotin and CD11b-APC (all from Pharmingen, Alphen a/d Rijn, The Netherlands). In between all steps, cells were washed with PBS containing 1% BSA and 0.05% Na-azide.

Binding of anti-CD115-biotin was detected with streptavidin conjugated with PerCP-Cy5.5 (Pharmingen, Alphen a/d Rijn, The Netherlands). Red blood cells were lysed with shock-buffer, cells were fixed with 1% paraformaldehyde and measured with an LSRII (Becton Dickinson, Erembodegem, Belgium).

To obtain leukocyte profiles, the following gating strategy was applied: debris was gated out in a forward (FSC)/side scatter (SSC) plot and leukocytes minus debris were divided according to their CD11b expression (myeloid lineage: CD11b-pos; lymphoid lineage: CD11b-neg). CD11b-pos cells were then selected and using Ly6G expression and SSC, cells were divided in neutrophilic granulocytes (Ly6G-hi/SSC-hi), eosinophilic granulocytes (Ly6G-neg/SSC-hi) and a non-granulocyte population (Ly6G-neg/SSC-low). The non-granulocyte population was then selected and using their CD11b and CD115 expression, monocytes (CD11b-pos/CD115-pos) and NK cells (CD11b-med/CD115-neg) were identified. Next, the monocyte population was selected and using Ly6C expression and FSC, classical monocytes (Ly6C-hi/FSC-low), non-classical monocytes (Ly6C-low/FSC-low) and intermediate monocytes (Ly6C-med/FSC-low) were identified. Going back to the lymphoid lineage (CD11b-neg cell population), using Ly6C-expression, lymphocytes (Ly6C-low/FSC-low) and lymphoblasts (Ly6-ly6C-med/FSC-hi) were identified.

Plasma lipids, lipoprotein profile, hepatic VLDL-TG production and liver lipids analysis

Plasma total cholesterol (TC), triglycerides (TG) and phospholipids (PL) levels were determined using enzymatic kits from Roche Molecular Biochemicals (Woerden, The Netherlands) according to the manufacturer's protocols. We used the following formula to calculate the cumulative plasma TC levels over 24 weeks of Western-type diet feeding which equals the area

under the curve for the plasma TC in time: $4*TC_{t=0} + 0.5*4*(TC_{t=4} - TC_{t=0}) + 4*TC_{t=4} + 0.5*4*(TC_{t=8} - TC_{t=4}) + 4*TC_{t=8} + 0.5*4*(TC_{t=12} - TC_{t=8}) + 4*TC_{t=12} + 0.5*4*(TC_{t=16} - TC_{t=12}) + 4*TC_{t=16} + 0.5*4*(TC_{t=20} - TC_{t=16}) + 4*TC_{t=20} + 0.5*4*(TC_{t=24} - TC_{t=20})$. The correlation between cumulative plasma TC level and atherosclerotic lesion area was assessed for both *E3L* and *E3L.LIKK* mice. For the determination of lipid distribution over plasma lipoproteins, pooled plasma per group was size-fractionated using an ÄKTA fast performance liquid chromatography (FPLC) system (Pharmacia, Roosendaal, The Netherlands). Each sample was injected onto a Superose 6 HR3.2/30 column and eluted at a constant flow rate of 50 µL/min in PBS, pH 7.4. Fractions of 50 µL were collected and assayed for TC as described above.

Mice were fasted for 4 hours prior to the start of the hepatic VLDL-TG production experiment, and, subsequently, sedated with 6.25 mg/kg acepromazine (Alfasan), 6.25 mg/kg midazolam (Roche), and 0.3125 mg/kg fentanyl (Janssen-Cilag). At timepoint zero, blood was taken via tail bleeding and mice were i.v. injected with 100 µL PBS containing 100 µCi Trans^{35}S label to measure *de novo* total apolipoprotein B (apoB) synthesis. After 30 min., the animals received 500 mg of tyloxapol (Triton WR-1339, Sigma-Aldrich) per kg body weight as a 10% (w/w) solution in sterile saline, to prevent systemic lipolysis of newly secreted hepatic VLDL-TG.[16] Additional blood samples were taken at regular timepoints after tyloxapol injection and used for determination of plasma TG concentration. At timepoint 120 min., the animals were sacrificed and blood was collected by orbital puncture for isolation of VLDL by density gradient ultracentrifugation.[17] ^{35}S-labeled total apoB content was measured in the VLDL fraction after precipitation with isopropanol.[18]

Lipids from liver tissue were extracted according to a protocol adapted from Bligh and Dyer.[19] Hepatic TG, PL concentrations were determined using the enzymatic kits as described previously. TC, free cholesterol (FC) and cholesteryl ester (CE) content were assessed with a cholesterol/cholesteryl ester quantitation enzymatic kit according to manufacturer's specifications (Biovision Research Products, Mountain View, CA). Liver lipids were expressed per mg protein, which was measured using the BCA protein assay kit (Pierce, Rockford, IL).

Atherosclerosis quantification

Mice were euthanized by carbon dioxide inhalation after 24 weeks of diet. Hearts were isolated and fixed in 4% paraformaldehyde, dehydrated and embedded in paraffin, and were cross-sectioned (5 µm) throughout the entire aortic root area. Of each mouse, 4 sections with 50-µm intervals were used for quantification of atherosclerotic lesion area. Characterization of lesion severity was performed separately in each of the 3 segments between the aortic valves in the 4 sections.[20]

Sections were stained with hematoxylin-phloxine-saffron (HPS). Atherosclerotic lesions were categorized for severity by one blinded observer, according to the guidelines of the American Heart Association, adapted for mice. Various types of lesions were distinguished: type 0 (no lesions) (Supplemental Fig. 8A), type I to III (early fatty streak-like lesions containing foam cells) (Supplemental Fig. 8B-D), and type IV to V (advanced lesions containing foam cells in the media, presence of fibrosis, cholesterol clefts, mineralization, and/or necrosis) (Supplemental Fig. 8E-F).

Immunohistochemistry for determination of adhering monocytes and macrophage-, and smooth muscle cell content in the lesions was performed as described previously.[21,22] The sections were incubated overnight with antibody M18 (1:100, Santa Cruz Biotechnology, Santa Cruz, Calif) and, subsequently, with biotinylated rabbit anti-goat conjugate (1:400, Brunschwig chemie, Amsterdam, The Netherlands) for quantification of MCP-1. AIA 31240 rabbit antiserum (1:1000, Accurate Chemical and Scientific, Westbury, NY) in combination with biotinylated donkey anti-rabbit conjugate (1:3000, Amersham Pharmacia Biotech) were used for quantification of both the number of monocytes adhering to the endothelium as well as the macrophage area. Antibody M0851 (1:800, Dako, Carpinteria, CA) and biotinylated horse anti-mouse conjugate (1:400, Vector Laboratories, Burlingame, CA) were used to quantify smooth muscle actin. Immunostaining was amplified using Vector Laboratories Elite ABC kit (Vector Laboratories, Burlingame, CA) and the immunoperoxidase complex was visualized with Nova Red (Vector Laboratories, Burlingame, CA). Counterstaining was performed with Mayer's hematoxylin. Sirius red was used to stain for collagen in the lesions (Chroma, Stuttgart, Germany).

Total lesion size, MCP-1-, macrophage-, smooth muscle cell-, and collagen content were quantified using Cell^D image analysis software (Olympus Soft Imaging Solutions, Münster, Germany).

Statistical analysis

Data are presented as means ±SEM. SPSS 17.0 for Windows (SPSS, Chicago, Ill) was used for statistical analysis. Statistical differences were assessed with the Mann-Whitney *U* test. For lesion typing, differences were determined by the χ^2 test. To assess the correlation between cumulative cholesterol exposure and atherosclerotic lesion area, the Pearson correlation test was performed after log transformation of the atherosclerotic lesion area. Differences at $P<0.05$ were regarded as statistically significant.

Results

LIKK causes low-grade inflammation

The overall appearance of *E3L* and *E3L.LIKK* mice during the study was similar. To assess whether expression of *LIKK* affects body weight gain, we measured food intake and body weight weekly. Both were not different between *E3L.LIKK* and *E3L* control mice (Supplemental Fig. 1A-B). The liver- and spleen weight and histological morphology of the liver were also comparable between *E3L.LIKK* and *E3L* mice (data not shown). To gain more insight in the effects of *LIKK* on inflammation, we determined whether *LIKK* expression increased the inflammatory state of the liver and systemic inflammatory markers in *E3L.LIKK* mice on a Western-type diet. We confirmed previous findings[15] showing that the enhanced expression of hepatocyte-specific human IKKβ (Supplemental Fig. 2A) resulted in a 1.4-fold increased hepatic NF-κB activation, as shown by an increase in the phosphorylated p65 subunit (pNF-κB^{Ser536}) (Supplemental Fig. 2B). IKKβ kinase phosphorylates subunit p65 of NF-κB at the position Ser536, which activates the transcriptional activity of NF-κB.[23] The transgenic expression of human IKKβ mRNA was present only in *E3L.LIKK* mice and did not alter murine IKKβ mRNA expression (Supplemental Fig. 2C-D). The enhanced

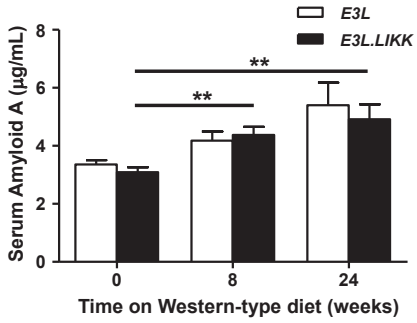

Fig. 1. *LIKK* does not increase plasma SAA levels. SAA levels were determined in plasma from *E3L.LIKK* (black bars) and *E3L* (white bars) mice fed a Western-type diet for 0, 8 and 24 weeks. Values are means ±SEM; n=15/group; ***P*<0.01.

hepatic NF-κB activation in *E3L.LIKK* mice did not result in increased IL-6 expression in whole liver, but did result in a tendency towards increased IL-1β expression (*P*=0.085) and a significant increase in MCP-1 expression (Supplemental Table 2).

To evaluate whether the increased hepatocyte-specific NF-κB activation in *E3L.LIKK* mice enhanced the systemic inflammatory state, we determined the plasma inflammation marker SAA and plasma cytokines under basal conditions. *LIKK* expression did not affect SAA before (3.1 ±0.17 *vs*. 3.4 ±0.15 µg/mL) and after 8 weeks (4.4 ±0.28 *vs*. 4.2 ±0.31 µg/mL) and 24 weeks (4.9 ±0.51 *vs*. 5.4 ±0.78 µg/mL) of Western-type diet feeding (Fig. 1), and neither the determined plasma cytokine levels (Supplemental Fig. 3A-F). SAA levels increased with Western-type diet feeding in both *E3L* and *E3L.LIKK* mice, but this difference only reached statistical significance in *E3L.LIKK* mice (Fig. 1).

Since we did not observe a clear increased systemic pro-inflammatory state under basal conditions, we challenged the mice with LPS to boost the inflammatory response. Interestingly, after injection of LPS, pro-inflammatory cytokines (*e.g.* IL-1β, IFNγ) showed a tendency towards increased plasma levels in *E3L.LIKK* mice as compared to *E3L* mice (Fig. 2A-F). The anti-inflammatory IL-10:IL-1β ratio was significantly lower in *E3L.LIKK* mice (Fig. 2G). Overall, these data indicate that *E3L.LIKK* mice are more sensitive to pro-inflammatory triggers compared to their *E3L* littermates.

To study whether this chronic low-grade inflammation in *E3L.LIKK* mice also resulted in increased inflammatory cell counts in liver and plasma, we determined the hepatic mRNA expression of various cell-type markers of inflammatory cells present in the liver, which are likely to influence atherogenesis,[24] and the number of circulating monocytes. Hepatic mRNA expression of CD68 (Kupffer cells), CD3 ((NK)T cells), and Vα14 (NKT cells) were not different between the genotypes (Supplemental Table 2), neither were the total number of circulating monocytes, the pro-inflammatory Ly6C-hi monocyte subset, the intermediate Ly6C-med monocyte subset and the less inflammatory Ly6C-lo monocyte subset (Supplemental Fig. 4A-D). Together, the above findings indicate that the enhanced hepatocyte-specific NF-κB activation

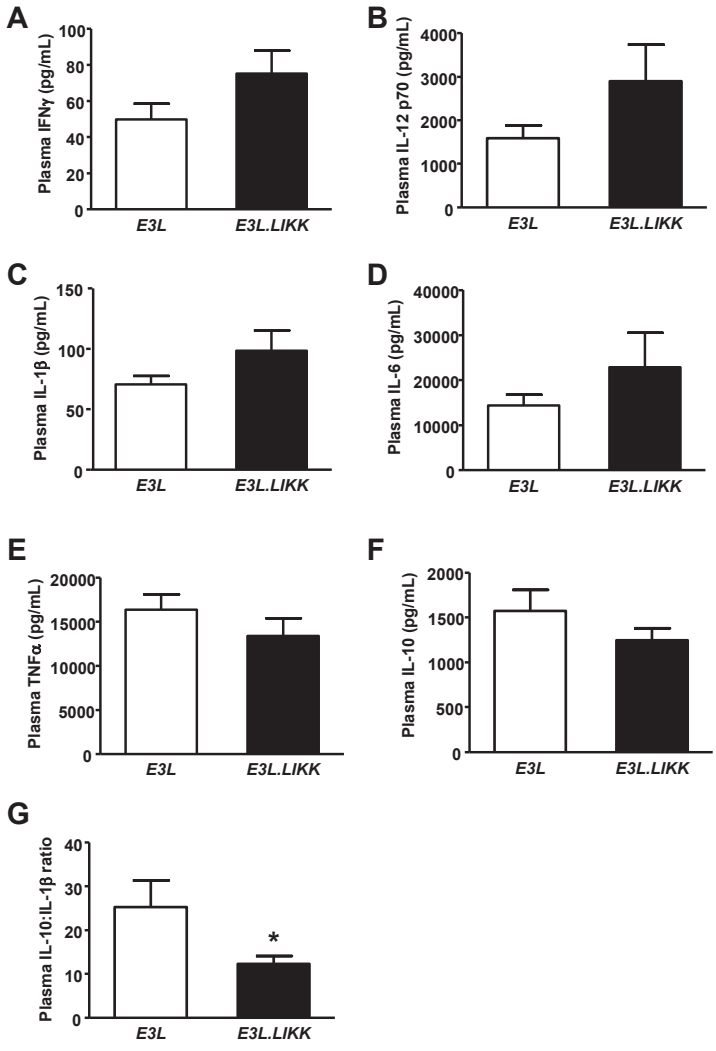

Fig. 2. *LIKK* tends to enhance plasma cytokines after LPS stimulation. LPS was injected intravenously in *E3L.LIKK* (black bars) and *E3L* (white bars) mice. Cytokine levels were measured 90 minutes after LPS injection (A-F). The IL-10:IL-1β ratio was calculated (G). Values are means ±SEM; n=7/group; **P*<0.05.

in *E3L.LIKK* mice results in a tendency towards a mildly enhanced hepatic pro-inflammatory state and an elevated sensitivity to pro-inflammatory stimuli as compared to *E3L* littermates.

LIKK transiently enhances VLDL cholesterol levels

To assess the effect of hepatocyte-specific NF-κB activation on plasma lipid levels, TC, TG and PL concentrations were determined every 4 weeks in *E3L.LIKK* and *E3L* mice. *LIKK* expression caused a transient increase of plasma TC levels only at 8 weeks (+50%; *P*<0.0001) and 12 weeks

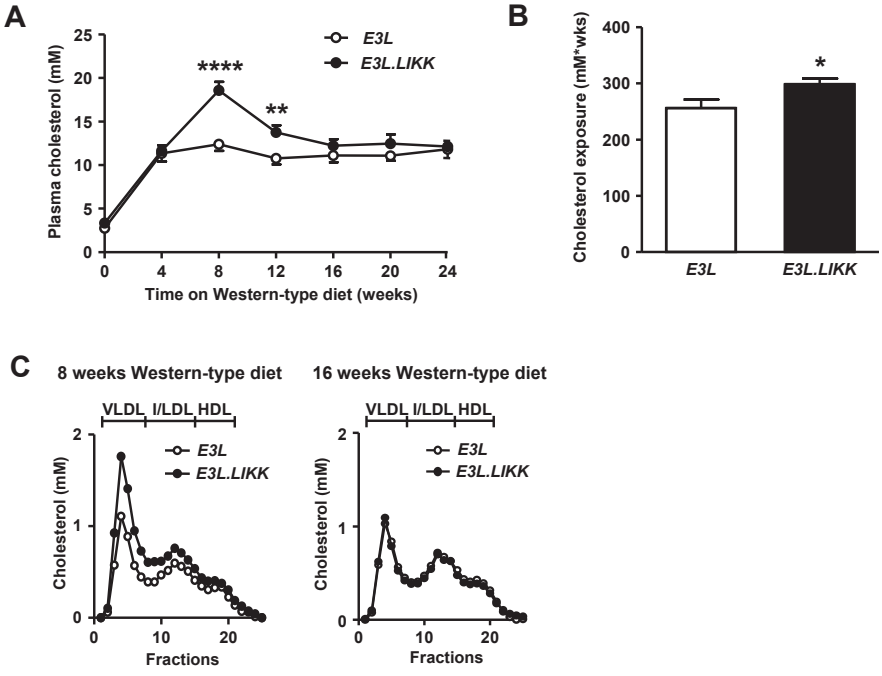

Fig. 3. *LIKK* transiently increases (V)LDL. Plasma cholesterol levels of *E3L.LIKK* (black symbols) and *E3L* (white symbols) mice fed a Western-type diet were assessed (A), and cumulative total cholesterol exposure was calculated (B). Lipoprotein profiles were determined at 8 (left) and 16 (right) weeks (C). Values are means ±SEM; n=15/group; **P*<0.05, ***P*<0.01, *****P*<0.0001.

(+28%; *P*<0.05) of Western-type diet feeding (Fig. 3A). Accordingly, the cumulative total cholesterol exposure was higher in *E3L.LIKK* than in *E3L* mice (+17%; *P*<0.05; Fig. 3B). A similar transient increase was found for plasma TG and PL levels (Supplemental Fig. 5A-B).

To determine which lipoproteins contribute to the transient elevated plasma TC levels, lipoproteins were size-fractionated by FPLC, and cholesterol was measured in the individual fractions. The transient increase in plasma TC levels at 8 weeks of Western-type diet feeding in *E3L.LIKK* mice was confined to (V)LDL, whereas at 16 weeks the lipoprotein distribution in the *E3L.LIKK* mice was similar to that of the *E3L* mice, in line with the plasma lipid levels (Fig. 3C). Consistent with our previous finding that expression of *LIKK* increased the VLDL production in male mice on chow diet,[15] we found that expression of *LIKK* increased, albeit not significantly, the VLDL-TG production rate (+24%) (Supplemental Fig. 6A), and tended to increase the VLDL-apolipoprotein B (apoB) production rate (+33%) (Supplemental Fig. 6B). No differences were observed in the liver lipid content between *E3L.LIKK* and *E3L* mice (Supplemental Fig. 7A-E). Taken together, these findings indicate that hepatocyte-specific NF-κB activation results in a modest and transient increase in plasma lipid levels in *E3L* mice.

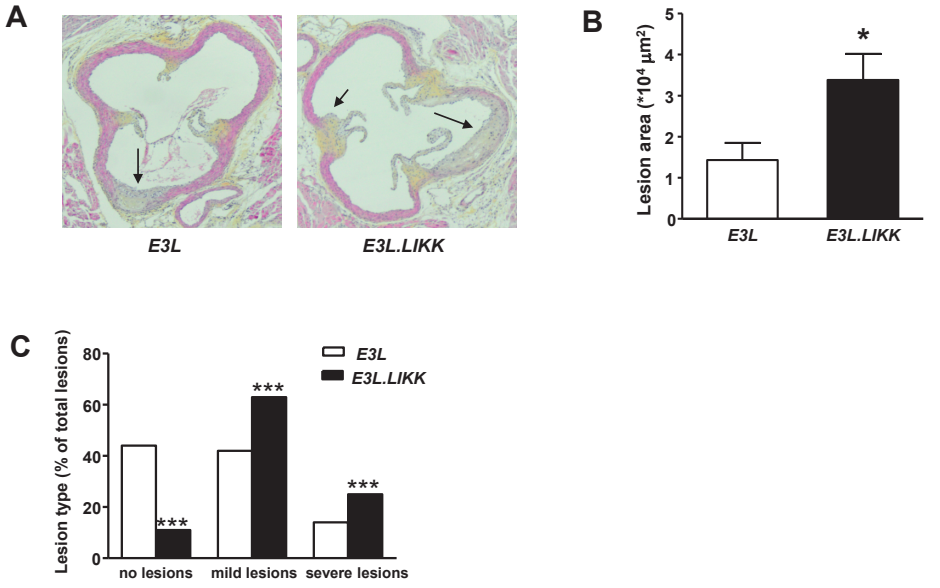

Fig. 4. *LIKK* aggravates atherosclerotic lesion area and severity. After 24 weeks of Western-type diet feeding, *E3L.LIKK* (black bars) and *E3L* (white bars) mice were sacrificed and cross-sections of aortic roots were stained with HPS. Representative pictures are shown. Arrows indicate lesions (A). Total lesion area was assessed in 4 sections of the aortic root (B) and lesion severity was determined separately in each of the 3 segments between the aortic valves of the 4 sections (C). Statistical analysis for lesion area was performed using the Mann-Whitney *U* test, and for lesion severity the χ^2 test. Values are means ±SEM; n=15/group; **P*<0.05, ****P*<0.001.

LIKK enhances atherosclerosis development

To investigate the effect of *LIKK* expression on atherosclerosis development, *E3L.LIKK* and *E3L* mice were sacrificed after 24 weeks of Western-type diet feeding, and lesion size and severity were measured in the aortic root. Representative pictures of both groups are shown in Fig. 4A. *E3L.LIKK* mice developed more than 2-fold larger atherosclerotic lesions (+131%; *P*<0.05; Fig. 4B) as compared to their *E3L* littermates. This increased lesion area coincided with more advanced lesion progression, since we found markedly fewer segments without atherosclerotic lesions (11% *vs*. 42%; *P*<0.001) and more segments with mild (63% *vs*. 44%; *P*<0.001) and severe lesions (26% *vs*. 14%; *P*<0.001) as compared to *E3L* mice (Fig. 4C). Examples of mild and severe lesions are shown in Supplemental Figure 8. These data indicate that chronic hepatocyte-specific NF-κB activation severely augments atherosclerosis development in *E3L* mice.

LIKK aggravates atherosclerotic lesion composition

We next evaluated whether *LIKK* expression would affect monocyte adherence and recruitment to the vascular wall, as well as the composition of the atherosclerotic lesions with respect to the macrophage, smooth muscle cell, and collagen content of the lesions. Adherence of monocytes to the vessel wall and the content of the chemokine monocyte chemoattractant protein-1

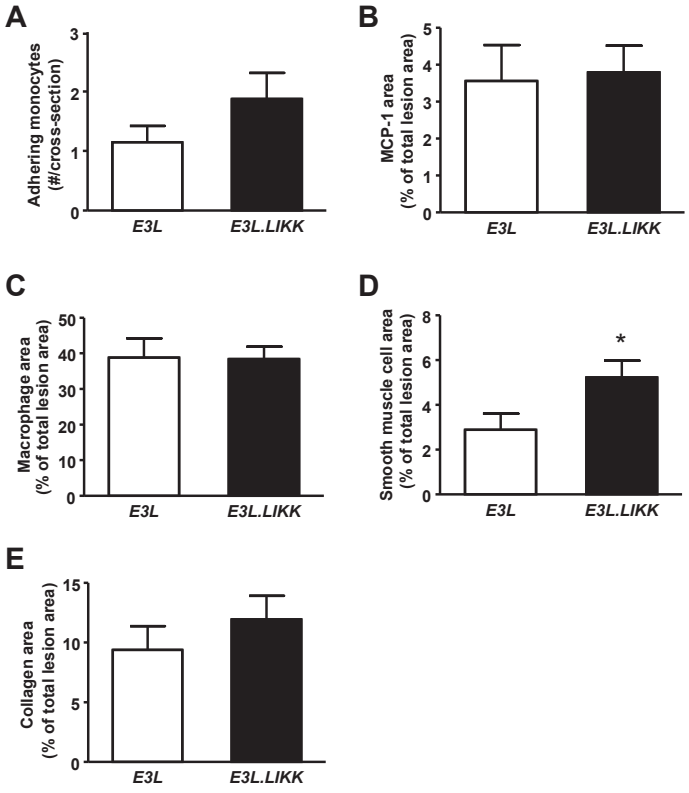

Fig. 5. *LIKK* induces more advanced atherosclerotic lesions. In the sections obtained as described in Fig. 4, the number of adhering monocytes (A), monocyte chemoattractant protein-1 (MCP-1) content (B), macrophage content (C), smooth muscle content (D) and collagen content (E) was determined. Values are means ±SEM; n=15/group; **P*<0.05, ***P*<0.01.

(MCP-1) of the atherosclerotic lesions were not significantly enhanced in *E3L.LIKK* mice as compared to *E3L* mice (Fig. 5A-B). *LIKK* expression did not affect the relative macrophage and collagen content of the lesions (Fig. 5C+E), but did result in an increased smooth muscle cell content of the lesions (+79%, *P*<0.05; Fig. 5D).

Aggravated atherosclerosis development in *E3L.LIKK* mice does not solely depend on the transient increase in plasma cholesterol levels

In *E3L* mice on Western-type diet, the cumulative plasma cholesterol exposure is highly predictive for the atherosclerotic lesion area (unpublished data, J.F.P. Berbée, P.C.N. Rensen). To verify if the transient increase in plasma TC levels (Fig. 3) alone could account for the aggravation in atherosclerosis development observed in *E3L.LIKK* mice, or whether additional mechanism(s) could contribute, including the low-grade systemic inflammation, we assessed the correlation between the cumulative plasma total cholesterol exposure and the atherosclerotic lesion area of the *E3L.LIKK* and *E3L* mice. As expected, there was a significant positive logarithmic correlation

between the atherosclerotic lesion area and the cumulative plasma cholesterol exposure in the control *E3L* mice (Supplemental Fig. 9A; r^2=0.757, *P*=0.002). However, we did not observe such a correlation in the *E3L.LIKK* mice (Supplemental Fig. 9B; r^2=-0.250, *P*=0.369), indicating that in addition to the transient increase in plasma TC levels in *E3L.LIKK* mice, additional mechanism(s), most likely the increased sensitivity to pro-inflammatory stimuli, contributed to the aggravated atherosclerosis development in these mice.

Discussion

NF-κB is regarded as a potential therapeutic target in atherosclerosis[3, 4] and studying tissue- and cell-specific effects of NF-κB in atherogenesis will expand our knowledge in the comprehensive actions of NF-κB on atherosclerosis development. The present study demonstrates for the first time that chronic, hepatocyte-specific expression of IKKβ (*LIKK*) and subsequent activation of NF-κB aggravates atherosclerosis development in *E3L* mice. In addition, the atherosclerotic lesion composition with respect to the macrophage and collagen content was not affected by *LIKK*, but in line with the presence of more advanced lesions, the smooth muscle cell content was increased. Expression of *LIKK* resulted in transiently increased plasma cholesterol levels and an enhanced sensitivity to pro-inflammatory triggers, which both are likely to have contributed to the increased atherosclerotic lesion size and severity. Since lesion size and severity are often correlated in atherosclerosis studies with different murine models,[13, 25] the increased lesion severity in *E3L.LIKK* mice is likely to be mainly attributed to the larger size of the lesions.

Expression of *LIKK* in *E3L* mice increased the activation of the NF-κB pathway in the liver, in line with our previous report.[15] In addition, hepatic mRNA expression of inflammatory parameters was increased or tended to be increased in *E3L.LIKK* mice, indicating that inflammatory mediators at local tissue level were enhanced in *E3L.LIKK* mice. This enhanced activation of hepatocyte-specific NF-κB in *E3L.LIKK* mice, however, did not result in a significant increased systemic pro-inflammatory state under basal conditions as compared to their *E3L* littermates. Importantly, Cai *et al*.[12] demonstrated that in *LIKK* mice on a wild-type background, systemic levels of IL-6 were only mildly elevated, while IL-1β and TNFα levels were similar as in wild-type mice. Our results show that *LIKK* expression on an *E3L* background resulted in a less pronounced hepatic inflammatory state as compared to *LIKK* expression on a wild-type background as described by Cai *et al*.,[12] as reflected in a smaller increase in active NF-κB (1.4- *vs*. 2.2-fold) and mRNA levels of pro-inflammatory cytokines levels in the liver. Furthermore, under basal conditions *E3L* mice have lower levels of active NF-κB present in the liver as compared to wild-type mice (unpublished data, J.A. van Diepen, M.C. Wong, P.J. Voshol). This implies that *E3L* mice have a lower chronic inflammatory state than wild-type mice, which could interfere with the pro-inflammatory effects caused by expression of *LIKK* in the present study. Also, in comparison with other murine atherosclerosis models, *e.g*. the *apoe*$^{-/-}$ and *ldlr*$^{-/-}$ mice, *E3L* mice display a milder phenotype with respect to hyperlipidemia and increased inflammation.[26, 27] In the current study, basal circulating levels of some cytokines were at borderline of the detection limit of current assays (Supplemental Fig. 3) and, as expected, the cytokine levels increased approximately 5- to 3700-fold after LPS injection (Fig. 2). Furthermore, after stimulation with

LPS, *E3L.LIKK* mice showed a tendency towards a higher systemic inflammatory state than *E3L* mice.

There is a strong interaction between inflammation and lipid metabolism.[28] For example, lowering inflammation using salicylate did not only reduced NF-κB activation, but concomitantly also reduced circulating cholesterol levels in *E3L* mice.[29] In line with this observation, in the present study we found higher plasma lipid levels at 8 weeks of Western-type diet feeding in female *E3L.LIKK* compared to *E3L* mice, which were confined to (V)LDL. We hypothesize that the increased lipid levels at this time point are accompanied by increased systemic inflammation, which is in line with previous findings showing that lipid metabolism and inflammation strongly influence each other.[28] A possible cause for the increased plasma lipid levels at 8 weeks of diet is therefore a more enhanced inflammation in the liver, possibly due to an increased activation of the NF-κB pathway in the liver.

We recently reported that male *E3L.LIKK* mice on chow diet also showed enhanced (V)LDL levels as a result of an increased hepatic VLDL-TG production rate,[15] and found in the current study a trend towards an enhanced VLDL-apoB production in female *E3L.LIKK* mice on Western-type diet, with a similar effect-size. Possible reasons for the less apparent increase of VLDL-TG production in females compared to males are differences in gender and/or diet. Although the increase in VLDL-TG production is more apparent in male *E3L.LIKK* mice, we used female mice in the present study. The main reason for this is that female *E3L* mice are more susceptible to develop atherosclerosis. In order for male *E3L* mice to become similarly atherosclerosis-prone they need to be fed Western-type diets not only with higher percentages of cholesterol, but also containing cholate. In addition, fructose was added to the drinking water to further raise their (V)LDL-cholesterol levels.[30] The increase in (V)LDL levels in females in the current study was only transient at 8 weeks of Western-type diet feeding and disappeared at 16 weeks. Since no differences in plasma lipid levels and hepatic mRNA expression of genes involved in lipid metabolism were detected between both groups at 24 weeks of diet, the increased VLDL-TG production at 8 weeks of diet is likely to be transient. At present, we cannot explain the transient nature of this increase in (V)LDL levels, but it may be the result of a progressive negative feedback mechanism to reduce the hepatic VLDL production which takes place during long-term Western-type diet feeding.

Dyslipidemia is regarded as the classical risk factor for atherosclerosis development. The transiently enhanced total cholesterol levels, resulting in a modest increase (+17%) in cumulative total cholesterol exposure upon *LIKK* expression, thus likely contributed to the enhanced atherosclerosis development. Previous diet-induced atherosclerosis studies in *E3L* mice have consistently demonstrated that there is a positive logarithmic relation between the cumulative cholesterol exposure during the study and the atherosclerotic lesion area (J.F.P. Berbée, P.C.N. Rensen, unpublished data). In agreement with these previous observations, we did observe such a significant logarithmic relation in *E3L* mice but not in *E3L.LIKK* mice. This suggests that the increase in atherosclerotic lesion area in *E3L.LIKK* mice can only partly be attributed to the transiently enhanced plasma cholesterol levels and that additional mechanisms are involved.

Inflammation is the second main risk factor for atherosclerosis. Enhanced extravascular or systemic inflammation, by the periodontal pathogen *Porphyromonas gingivalis*[31] or by repeated

administration of LPS,[21] respectively, promotes atherosclerosis development. In addition, in humans, low-grade systemic inflammation is associated with enhanced risk of coronary artery disease.[32,33] It is thus likely that, as discussed above, the increased sensitivity for pro-inflammatory triggers such as LPS in *E3L.LIKK* mice also directly contributed to the enhanced atherosclerotic lesion formation.

We excluded higher circulating levels of pro-inflammatory Ly6C-hi monocytes as being another possible contributor to the aggravated atherosclerosis development in *E3L.LIKK* mice. Adhesion of monocytes to endothelial cells and subsequent migration into the vessel wall is one of the crucial steps in atherosclerotic lesion formation. Ly6C-hi monocytes are more prone to adhere to activated endothelium than Ly6C-lo monocytes and are, therefore, associated with enhanced atherosclerosis development.[34] We found that *E3L.LIKK* mice had similar levels of circulating subsets of monocytes as compared to their *E3L* controls, which is consistent with the observed similar number of adhering monocytes to the vascular wall.

In line with the enhanced atherosclerosis development that we observed in *E3L.LIKK* mice, Luchtefeld *et al.*[11] have reported that gp130-deficient mice with defective IL-6 signaling specifically in hepatocytes, develop less atherosclerosis, indicating that modulation of hepatic inflammation can have profound effects on atherogenesis. These studies also underscore that enhanced inflammation in the liver, *e.g.* due to viral hepatitis or steatohepatitis, may augment atherosclerosis development. Indeed, in several clinical studies, such hepatic pathological conditions are associated with an elevated occurrence of CVD.[35, 36, 37] Even after adjustment for classical risk factors for CVD, such as LDL cholesterol levels, chronic hepatitis C infection was still significantly associated with increased atherosclerosis in a cross-sectional study.[37] Together, these findings suggest that there is a direct effect of hepatic inflammation on atherosclerosis development, independent of systemic lipid levels. Moreover, they suggest that in addition to the currently used lipid-targeted drugs such as statins, reducing NF-κB activity in the liver may be a promising additive therapeutic strategy against atherosclerosis development.

In conclusion, we have shown that hepatocyte-specific activation of NF-κB leads to larger and more advanced atherosclerotic lesions. Our studies furthermore suggest that both the transient elevated (V)LDL cholesterol levels as well as the increased sensitivity to pro-inflammatory stimuli are most likely responsible for this aggravating effect on atherosclerosis. These findings contribute to the present understanding of the role of the liver, and more specifically the role of hepatic NF-κB, in atherosclerosis development and may help to develop new innovative anti-atherosclerotic strategies.

References

1. Libby P. Inflammation in atherosclerosis. *Nature*. 2002;420:868-874.
2. de Winther MP, Kanters E, Kraal G, Hofker MH. Nuclear factor kappaB signaling in atherogenesis. *Arterioscler Thromb Vasc Biol*. 2005;25:904-914.
3. Chiba T, Kondo Y, Shinozaki S, Kaneko E, Ishigami A, Maruyama N, Umezawa K, Shimokado K. A selective NFkappaB inhibitor, DHMEQ, reduced atherosclerosis in ApoE-deficient mice. *J Atheroscler Thromb*. 2006;13:308-313.
4. Cuaz-Perolin C, Billiet L, Bauge E, Copin C, Scott-Algara D, Genze F, Buchele B, Syrovets T, Simmet T, Rouis M. Antiinflammatory and Antiatherogenic Effects of the NF-kappaB Inhibitor Acetyl-11-Keto-beta-Boswellic Acid in LPS-Challenged ApoE-/- Mice. *Arterioscler Thromb Vasc Biol*. 2007;28:272-277.
5. Gareus R, Kotsaki E, Xanthoulea S, van der Made I, Gijbels MJ, Kardakaris R, Polykratis A, Kollias G, de Winther MP, Pasparakis M. Endothelial cell-specific NF-kappaB inhibition protects mice from atherosclerosis. *Cell Metab*. 2008;8:372-383.
6. Kanters E, Gijbels MJ, van der Made I, Vergouwe MN, Heeringa P, Kraal G, Hofker MH, de Winther MP. Hematopoietic NF-kappaB1 deficiency results in small atherosclerotic lesions with an inflammatory phenotype. *Blood*. 2004;103:934-940.
7. Kanters E, Pasparakis M, Gijbels MJ, Vergouwe MN, Partouns-Hendriks I, Fijneman RJ, Clausen BE, Forster I, Kockx MM, Rajewsky K, Kraal G, Hofker MH, de Winther MP. Inhibition of NF-kappaB activation in macrophages increases atherosclerosis in LDL receptor-deficient mice. *J Clin Invest*. 2003;112:1176-1185.
8. Lavoie JM, Gauthier MS. Regulation of fat metabolism in the liver: link to non-alcoholic hepatic steatosis and impact of physical exercise. *Cell Mol Life Sci*. 2006;63:1393-1409.
9. Knolle PA, Gerken G. Local control of the immune response in the liver. *Immunol Rev*. 2000;174:21-34.
10. Trautwein C, Boker K, Manns MP. Hepatocyte and immune system: acute phase reaction as a contribution to early defence mechanisms. *Gut*. 1994;35:1163-1166.
11. Luchtefeld M, Schunkert H, Stoll M, Selle T, Lorier R, Grote K, Sagebiel C, Jagavelu K, Tietge UJ, Assmus U, Streetz K, Hengstenberg C, Fischer M, Mayer B, Maresso K, El Mokhtari NE, Schreiber S, Muller W, Bavendiek U, Grothusen C, Drexler H, Trautwein C, Broeckel U, Schieffer B. Signal transducer of inflammation gp130 modulates atherosclerosis in mice and man. *J Exp Med*. 2007;204:1935-1944.
12. Cai D, Yuan M, Frantz DF, Melendez PA, Hansen L, Lee J, Shoelson SE. Local and systemic insulin resistance resulting from hepatic activation of IKK-beta and NF-kappaB. *Nat Med*. 2005;11:183-190.
13. Westerterp M, van der Hoogt CC, de HW, Offerman EH, linga-Thie GM, Jukema JW, Havekes LM, Rensen PC. Cholesteryl ester transfer protein decreases high-density lipoprotein and severely aggravates atherosclerosis in APOE*3-Leiden mice. *Arterioscler Thromb Vasc Biol*. 2006;26:2552-2559.
14. van Vlijmen BJ, van den Maagdenberg AM, Gijbels MJ, van der Boom H, HogenEsch H, Frants RR, Hofker MH, Havekes LM. Diet-induced hyperlipoproteinemia and atherosclerosis in apolipoprotein E3-Leiden transgenic mice. *J Clin Invest*. 1994;93:1403-1410.
15. van Diepen JA, Wong MC, Guigas B, Bos J, Stienstra R, Hodson L, Shoelson SE, Berbee JF, Rensen PC, Romijn JA, Havekes LM, Voshol PJ. Hepatocyte-specific IKK-beta activation enhances VLDL-triglyceride production in APOE*3-Leiden mice. *J Lipid Res*. 2011.
16. alto-Setala K, Fisher EA, Chen X, Chajek-Shaul T, Hayek T, Zechner R, Walsh A, Ramakrishnan R, Ginsberg HN, Breslow JL. Mechanism of hypertriglyceridemia in human apolipoprotein (apo) CIII transgenic mice. Diminished very low density lipoprotein fractional catabolic rate associated with increased apo CIII and reduced apo E on the particles. *J Clin Invest*. 1992;90:1889-1900.
17. Redgrave TG, Roberts DC, West CE. Separation of plasma lipoproteins by density-gradient ultracentrifugation. *Anal Biochem*. 1975;65:42-49.
18. Egusa G, Brady DW, Grundy SM, Howard BV. Isopropanol precipitation method for the determination of apolipoprotein B specific activity and plasma concentrations during metabolic studies of very low density lipoprotein and low density lipoprotein apolipoprotein B. *J Lipid Res*. 1983;24:1261-1267.
19. Bligh EG, Dyer WJ. A rapid method of total lipid extraction and purification. *Can J Biochem Physiol*. 1959;37:911-917.

20. Zadelaar AS, Boesten LS, Jukema JW, van Vlijmen BJ, Kooistra T, Emeis JJ, Lundholm E, Camejo G, Havekes LM. Dual PPARalpha/gamma agonist tesaglitazar reduces atherosclerosis in insulin-resistant and hypercholesterolemic ApoE*3Leiden mice. *Arterioscler Thromb Vasc Biol*. 2006;26:2560-2566.
21. Westerterp M, Berbée JF, Pires NM, van Mierlo GJ, Kleemann R, Romijn JA, Havekes LM, Rensen PC. Apolipoprotein C-I is crucially involved in lipopolysaccharide-induced atherosclerosis development in apolipoprotein E-knockout mice. *Circulation*. 2007;116:2173-2181.
22. de Haan W, de Vries-van der Weij J, van der Hoorn JW, Gautier T, van der Hoogt CC, Westerterp M, Romijn JA, Jukema JW, Havekes LM, Princen HM, Rensen PC. Torcetrapib does not reduce atherosclerosis beyond atorvastatin and induces more proinflammatory lesions than atorvastatin. *Circulation*. 2008;117:2515-2522.
23. Sasaki CY, Slemenda CF, Ghosh P, Barberi TJ, Longo DL. Traf1 induction and protection from tumor necrosis factor by nuclear factor-kappaB p65 is independent of serine 536 phosphorylation. *Cancer Res*. 2007;67:11218-11225.
24. Hansson GK, Hermansson A. The immune system in atherosclerosis. *Nat Immunol*. 2011;12:204-212.
25. Lutgens E, de Muinck ED, Heeneman S, Daemen MJ. Compensatory enlargement and stenosis develop in apoE(-/-) and apoE*3-Leiden transgenic mice. *Arterioscler Thromb Vasc Biol*. 2001;21:1359-1365.
26. Zadelaar S, Kleemann R, Verschuren L, de Vries-Van der Weij, van der HJ, Princen HM, Kooistra T. Mouse models for atherosclerosis and pharmaceutical modifiers. *Arterioscler Thromb Vasc Biol*. 2007;27:1706-1721.
27. Kleemann R, Verschuren L, van Erk MJ, Nikolsky Y, Cnubben NH, Verheij ER, Smilde AK, Hendriks HF, Zadelaar S, Smith GJ, Kaznacheev V, Nikolskaya T, Melnikov A, Hurt-Camejo E, van der GJ, van OB, Kooistra T. Atherosclerosis and liver inflammation induced by increased dietary cholesterol intake: a combined transcriptomics and metabolomics analysis. *Genome Biol*. 2007;8:R200.
28. Khovidhunkit W, Kim MS, Memon RA, Shigenaga JK, Moser AH, Feingold KR, Grunfeld C. Effects of infection and inflammation on lipid and lipoprotein metabolism: mechanisms and consequences to the host. *J Lipid Res*. 2004;45:1169-1196.
29. de Vries-van der Weij, Toet K, Zadelaar S, Wielinga PY, Kleemann R, Rensen PC, Kooistra T. Anti-inflammatory salicylate beneficially modulates pre-existing atherosclerosis through quenching of NF-kappaB activity and lowering of cholesterol. *Atherosclerosis*. 2010;213:241-246.
30. Trion A, de Maat MP, Jukema JW, van der LA, Maas MC, Offerman EH, Havekes LM, Szalai AJ, Princen HM, Emeis JJ. No effect of C-reactive protein on early atherosclerosis development in apolipoprotein E*3-leiden/human C-reactive protein transgenic mice. *Arterioscler Thromb Vasc Biol*. 2005;25:1635-1640.
31. Gibson FC, III, Yumoto H, Takahashi Y, Chou HH, Genco CA. Innate immune signaling and Porphyromonas gingivalis-accelerated atherosclerosis. *J Dent Res*. 2006;85:106-121.
32. Danesh J, Whincup P, Walker M, Lennon L, Thomson A, Appleby P, Gallimore JR, Pepys MB. Low grade inflammation and coronary heart disease: prospective study and updated meta-analyses. *BMJ*. 2000;321:199-204.
33. Fang L, Wei H, Mak KH, Xiong Z, Song J, Wang D, Lim YL, Chatterjee S. Markers of low-grade inflammation and soluble cell adhesion molecules in Chinese patients with coronary artery disease. *Can J Cardiol*. 2004;20:1433-1438.
34. Swirski FK, Libby P, Aikawa E, Alcaide P, Luscinskas FW, Weissleder R, Pittet MJ. Ly-6Chi monocytes dominate hypercholesterolemia-associated monocytosis and give rise to macrophages in atheromata. *J Clin Invest*. 2007;117:195-205.
35. Ishizaka N, Ishizaka Y, Takahashi E, Toda EE, Hashimoto H, Ohno M, Nagai R, Yamakado M. Increased prevalence of carotid atherosclerosis in hepatitis B virus carriers. *Circulation*. 2002;105:1028-1030.
36. Sookoian S, Pirola CJ. Non-alcoholic fatty liver disease is strongly associated with carotid atherosclerosis: a systematic review. *J Hepatol*. 2008;49:600-607.
37. Mostafa A, Mohamed MK, Saeed M, Hasan A, Fontanet A, Godsland I, Coady E, Esmat G, El-Hoseiny M, bdul-Hamid M, Hughes A, Chaturvedi N. Hepatitis C infection and clearance: impact on atherosclerosis and cardiometabolic risk factors. *Gut*. 2010;59:1135-1140.

Supplemental data

Supplemental Table 1. Primers used for RT-PCR.

Human target	**Forward primer**	**Reverse primer**
*IKK*β	GGAGCTCTGTGGGCGGGAGA	GGCCCATGGGGCTCCTCTGT
Murine target	**Forward primer**	**Reverse primer**
ApoB	GCCCATTGTGGACAAGTTGATC	CCAGGACTTGGAGGTCTTGGA
CD3	CTGTCTAGAGGGCACGTCAA	GATGCGGTGGAACACTTTCT
CD68	CCTCCACCCTCGCCTAGTC	TTGGGTATAGGATTCGGATTTGA
Cpt1a	GAGACTTCCAACGCATGACA	ATGGGTTGGGGTGATGTAGA
Cyclo	CAAATGCTGGACCAAACACAA	GCCATCCAGCCATTCAGTCT
Fas	TCCTGGGAGGAATGTAAACAGC	CACAAATTCATTCACTGCAGCC
Gapdh	TGCACCACCAACTGCTTAGC	GGCATGGACTGTGGTCATGAG
Hmgcr	CCGGCAACAACAAGATCTGTG	ATGTACAGGATGGCGATGCA
Hprt	TTGCTCGAGATGTCATGAAGGA	AGCAGGTCAGCAAAGAACTTATAG
*IKK*β	GCCCTCTGCTCCCGGCTAGA	CCAGTCTAGAGTCGTGAAGCTTCTGT
*IL-1*β	GCAACTGTTCCTGAACTCAACT	ATCTTTTGGGGTCCGTCAACT
IL-6	CCGGAGAGGAGACTTCACAG	TTCTGCAAGTGCATCATCGT
MCP-1	GCATCTGCCCTAAGGTCTTCA	TTCACTGTCACACTGGTCACTCCTA
MTTP	CTCTTGGCAGTGCTTTTTCTCT	GAGCTTGTATAGCCGCTCATT
Vα14	GTGGGTGGCTGGCAAGAC	TCTCCCTGACGCACAACCA
Srebp-1c	GGAGCCATGGATTGCACATT	GGCCCGGGAAGTCACTGT

IKKβ, IκB kinase-β; *Apob*, apolipoprotein B; *Cd3*, marker for (NK)T cells; *CD68*, marker for macrophages (Kupffer cells); *Cpt1a*, carnitine palmitoyltransferase 1a; *Cyclo*, cyclophilin; *Fas*, fatty acid synthase; *Gapdh*, glyceraldehyde-3-phosphate dehydrogenase; *Hmgcr*, HMG-CoA reductase; *Hprt*, hypoxanthine-guanine phosphoribosyl transferase; *IL-1β*, interleukin-1β; *IL-6*, interleukin-6; *MCP-1*, monocyte chemoattractant protein-1; *Mttp*, microsomal triglyceride transfer protein; *Srebp-1c*, sterol-regulatory element binding protein; *Vα14*, marker for NKT cells.

Supplemental Table 2. Expression of *LIKK* increases hepatic MCP-1 expression.

Target	*E3L*	*E3L.LIKK*	Significance
Cytokines and chemokines			
*IL-1*β	1.00 ± 0.05	1.24 ± 0.14	*P* = 0.085
IL-6	1.00 ± 0.13	1.24 ± 0.20	n.s.
MCP-1	1.00 ± 0.27	1.39 ± 0.32*	*P* = 0.049
Inflammatory cells			
CD68	1.00 ± 0.29	1.15 ± 0.14	n.s.
CD3	1.00 ± 0.14	0.69 ± 0.30	n.s.
Vα14	1.00 ± 0.08	0.94 ± 0.21	n.s.
VLDL secretion			
ApoB	1.00 ± 0.24	1.00 ± 0.33	n.s.
MTTP	1.00 ± 0.13	1.15 ± 0.28	n.s.
Lipogenesis			
Srebp-1c	1.00 ± 0.19	1.46 ± 0.49	n.s.
Fas	1.00 ± 0.21	0.83 ± 0.19	n.s.

After 24 weeks of Western-type diet, *E3L.LIKK* and *E3L* mice were sacrificed, livers were isolated and mRNA expression of indicated targets were quantified by RT-PCR. Data are calculated as fold difference as compared to the control group. Values are means ±SEM; n=6-15/group; *P<0.05 compared to the control group; n.s., not significant. *IKKβ*, IκB kinase-β; *Apob*, apolipoprotein B; *Cd3*, marker for (NK)T cells; *CD68*, marker for macrophages (Kupffer cells); *Cpt1a*, carnitine palmitoyltransferase 1a; *Cyclo*, cyclophilin; *Fas*, fatty acid synthase; *Gapdh*, glyceraldehyde-3-phosphate dehydrogenase; *Hmgcr*, HMG-CoA reductase; *Hprt*, hypoxanthine-guanine phosphoribosyl transferase; *IL-1β*, interleukin-1β; *IL-6*, interleukin-6; *MCP-1*, monocyte chemoattractant protein-1; *Mttp*, microsomal triglyceride transfer protein; *Srebp-1c*, sterol-regulatory element binding protein; *Vα14*, marker for NKT cells.

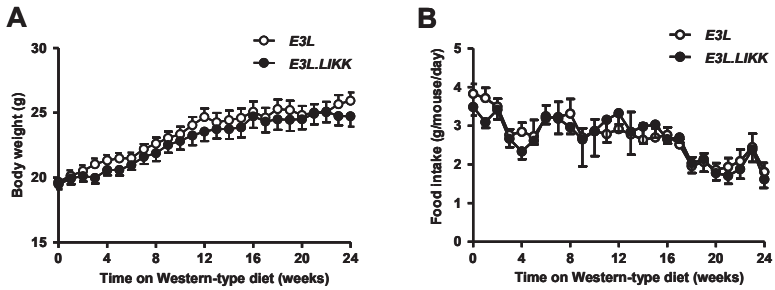

Supplemental Fig. 1. Expression of *LIKK* does not affect body weight and food intake. *E3L.LIKK* (black symbols) and *E3L* mice (white symbols) were fed a Western-type diet for 24 weeks. Body weight (A) and food intake (B) were measured weekly. Values are means ±SEM; n=15/group.

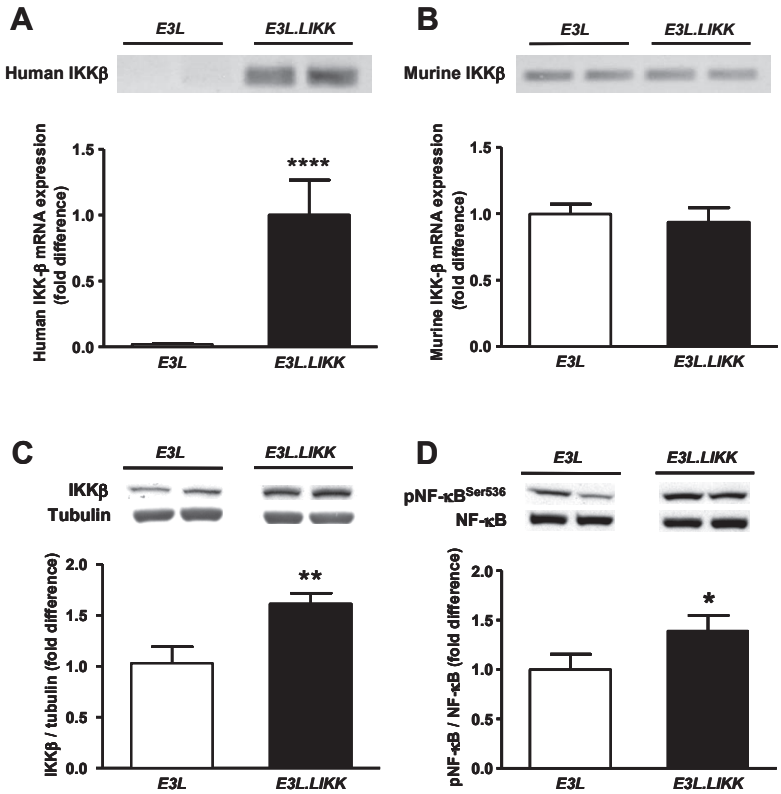

Supplemental Fig. 2. Expression of *LIKK* increases hepatic IKKβ mRNA and protein expression, and NF-κB protein activity. After 24 weeks of Western-type diet, *E3L.LIKK* (black bars) and *E3L* mice (white bars) were sacrificed, livers were isolated and hepatic mRNA expression of human IKKβ (A) and murine IKKβ (B) was quantified by RT-PCR. Human IKKβ is expressed as fold difference compared to *E3L.LIKK* mice and murine IKKβ to *E3L* mice. The inserts show representative bands of two mice per group of the qPCR product run on a gel. Values are mean ±SEM; n=14-15/group; ****P<0.0001. Hepatic protein expression of IKKβ normalized to tubulin (C) and phosphorylated NF-κB p65Ser536 normalized to total NF-κB (D) was assessed in *E3L.LIKK* (black bars) and *E3L* mice (white bars). Values are mean ±SEM; n=6-7/group; *P<0.05, **P<0.01.

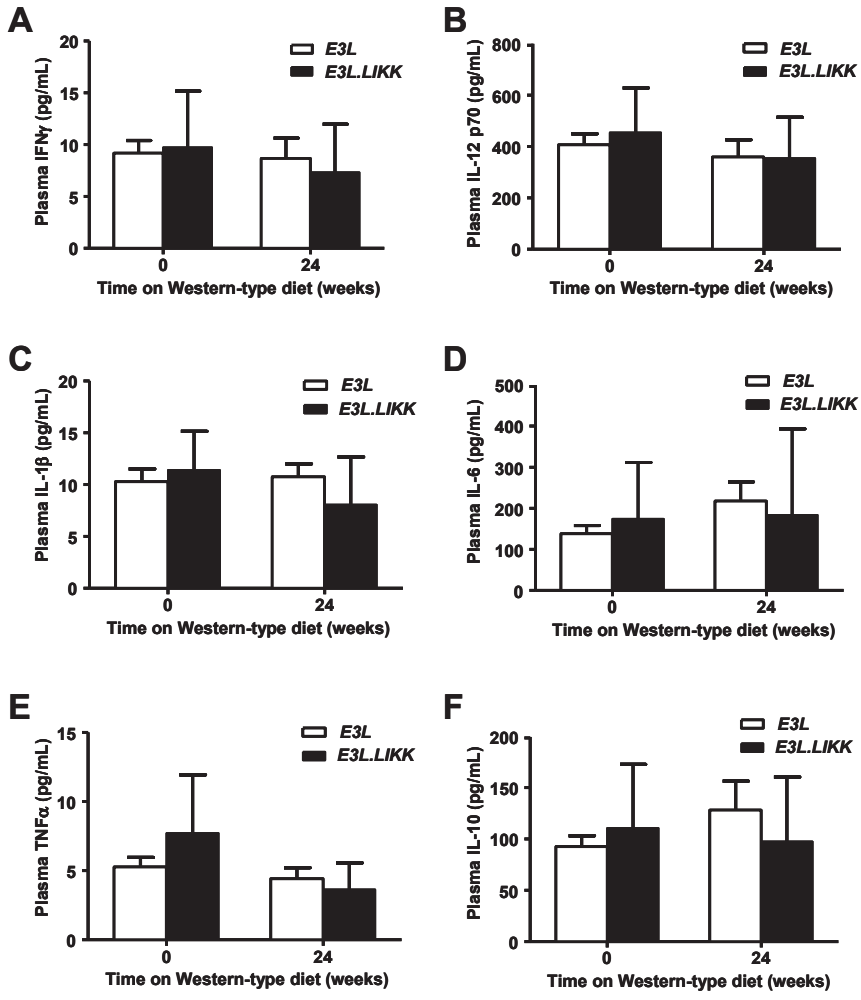

Supplemental Fig. 3. *LIKK* does not affect plasma cytokines after 0 and 24 weeks of diet. *E3L.LIKK* (black bars) and *E3L* (white bars) were fed 24 weeks of Western-type diet. Plasma levels of the indicated cytokines were measured at t=0 and 24 weeks of diet. Values are means ±SEM; n=15/group.

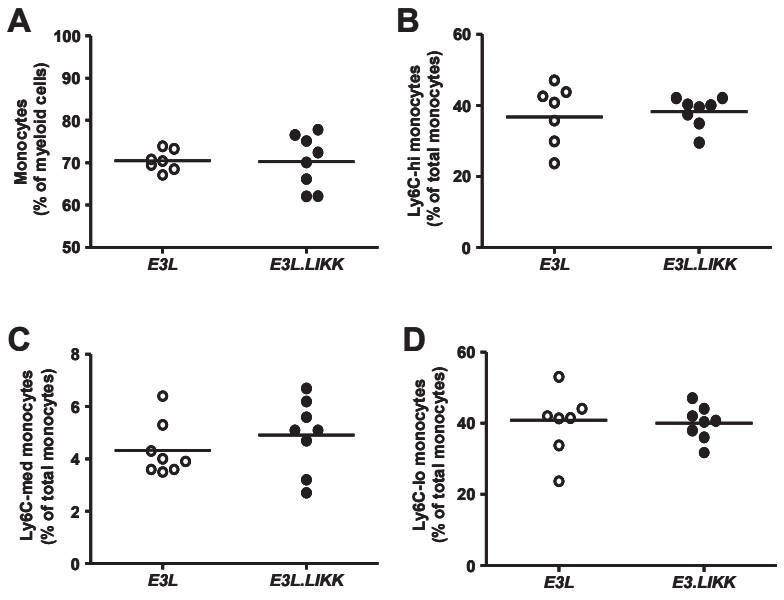

Supplemental Fig. 4. *LIKK* does not affect circulating subsets of monocytes. Blood was drawn from *E3L.LIKK* (black circles) and *E3L* (open circles) mice fed a Western-type diet for 8 weeks. The number of monocytes (A) and Ly6C-hi (B), Ly6C-med (C) and Ly6C-lo (D) expressing subsets were determined by FACS analysis. n=7-8/group.

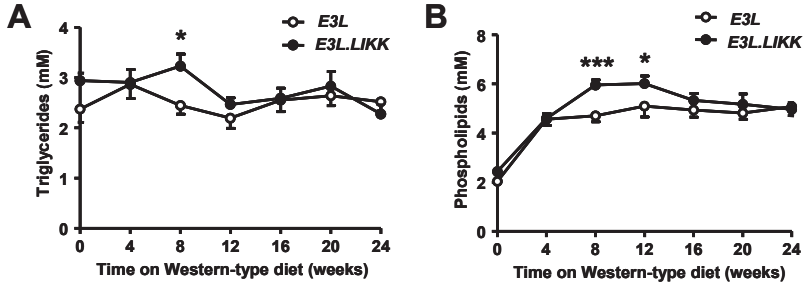

Supplemental Fig. 5. *LIKK* transiently increases plasma triglycerides and phospholipids. *E3L.LIKK* (black symbols) and *E3L* mice (white symbols) were fed a Western-type diet for 24 weeks. Plasma was obtained every 4 weeks to determine triglycerides (TG) (A) and phospholipids (PL) (B) concentration over time. Values are means ±SEM; n=15/group; **P*<0.05, ****P*<0.001.

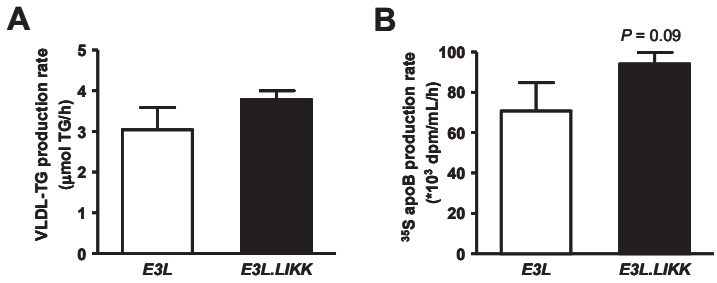

Supplemental Fig. 6. Expression of *LIKK* tends to increase VLDL-apoB production. After 8 weeks of Western-type diet, *E3L.LIKK* (black bars) and *E3L* mice (white bars) were fasted 4 hours and injected with Trans35S and tyloxapol, and blood samples were drawn after tyloxapol injection. The rate of TG production was calculated from the slopes of the curves from the individual mice (A). After 120 min, the total VLDL-fraction was isolated by ultracentrifugation, ^{35}S-activity was counted, and the production rate of newly synthesized VLDL-^{35}S-apoB was determined (B). Values are means ±SEM; n=5-11/group.

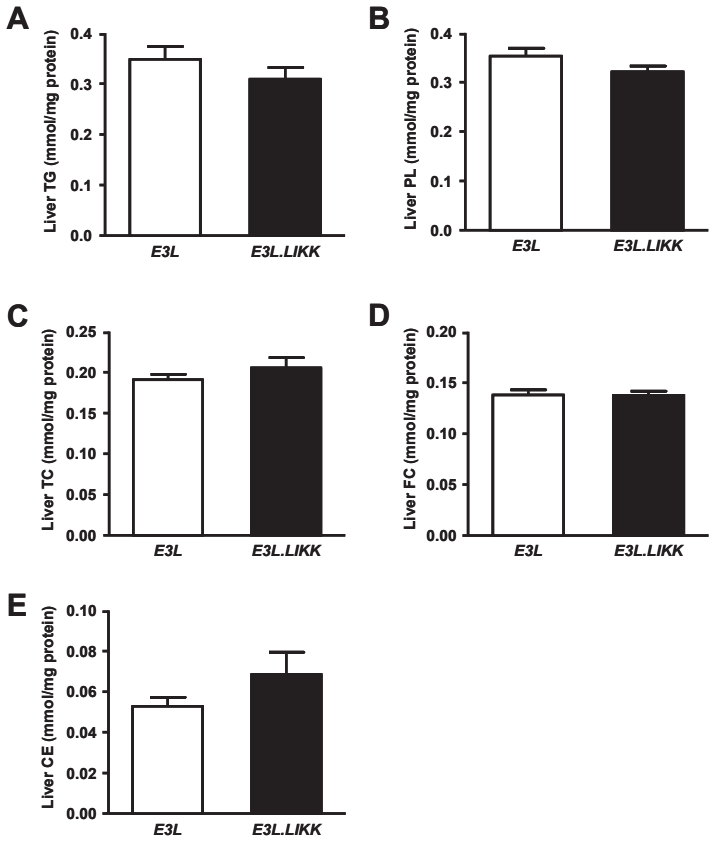

Supplemental Fig. 7. *LIKK* does not affect liver lipid content. After 24 weeks of Western-type diet, the livers of *E3L.LIKK* (black bars) and *E3L* mice (white bars) were isolated and triglyceride (TG) (A), phospholipid (PL) (B), total cholesterol (TC) (C), free cholesterol (FE) (D), cholesteryl ester (CE) (E) content was determined. Values are means ±SEM; n=14-15/group.

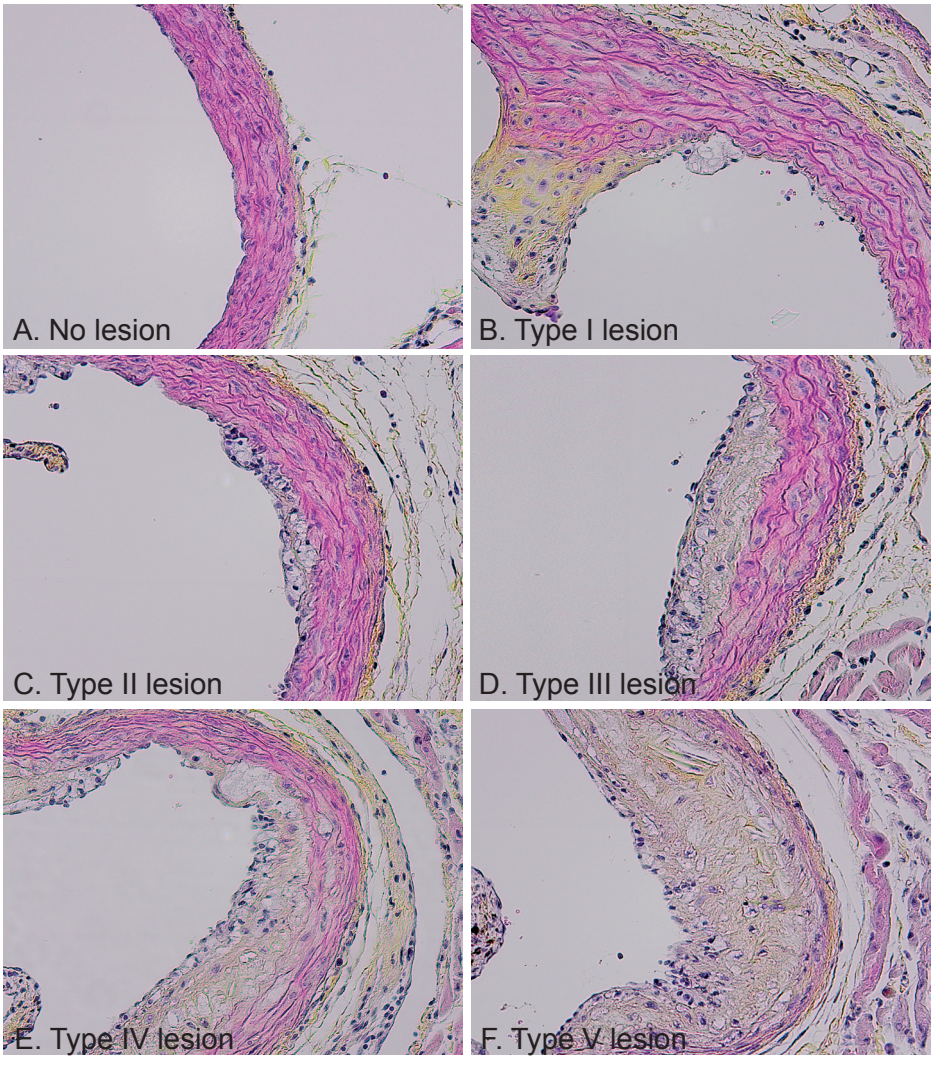

Supplemental Fig. 8. Representative pictures of HPS-stained segments classified in different severities. Atherosclerotic lesions are categorized into mild (type I-III) and severe (type IV-V) phenotypes. Magnification 200x. (A). No lesion. (B). Type I, early fatty streak: per section up to 10 foam cells present in the intima. (C). Type II, regular fatty streak: more than 10 foam cells present in the intima. (D). Type III, mild plaque: extension of foam cells into the media and covered by a fibrotic cap. (E). Type IV, moderate plaque: a more progressive lesion infiltrating into the media, fibrosis in the media, without loss of architecture. (F). Type V, severe plaque: the media is severely damaged, elastic lamina are broken, presence of cholesterol clefts, mineralization and/or necrosis.

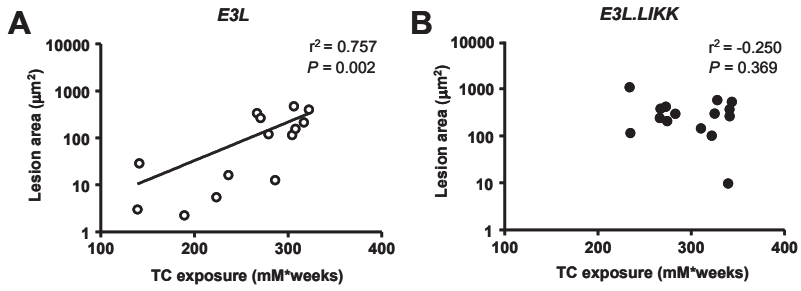

Supplemental Fig. 9. Correlation between cumulative plasma TC exposure and atherosclerotic lesion area. The correlation between the cumulative plasma TC exposure and atherosclerotic lesion area, after log transformation, in *E3L* (open circles) (A) and the *E3L.LIKK* mice (closed circles) (B) was determined using the Pearson correlation test. n=15/group.